

Manpower was committed in the RWP2020 (unit=F.T.E.). Manpower invested in the various Work Packages was reported (blue part) for the first half of 2020 (January-June 2012).

### Manpower (in F.T.E) in 2020 RWP Work Packages

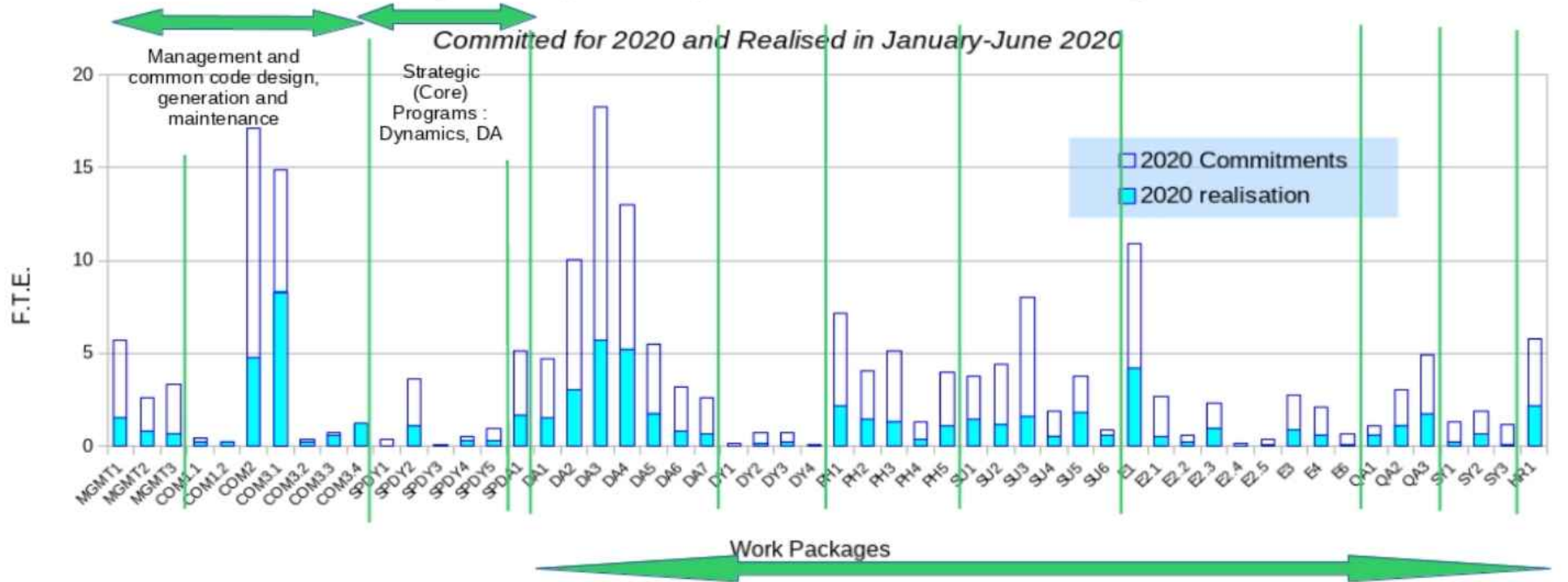


Prospective R&D activities :  
 Atmospheric data assimilation, Dynamics, Atmospheric physics parametrizations, Surface analysis and modelling, Probabilistic forecasting , Quality assessment and monitoring , Technical code and system development, Towards high-resolution modelling



**Manpower was committed in the RWP2020 (unit=F.T.E.). Manpower invested in the various Work Packages was reported (blue part) for the first half of 2020 (January-June 2020).**

### Manpower (in F.T.E) in 2020 RWP Work Packages

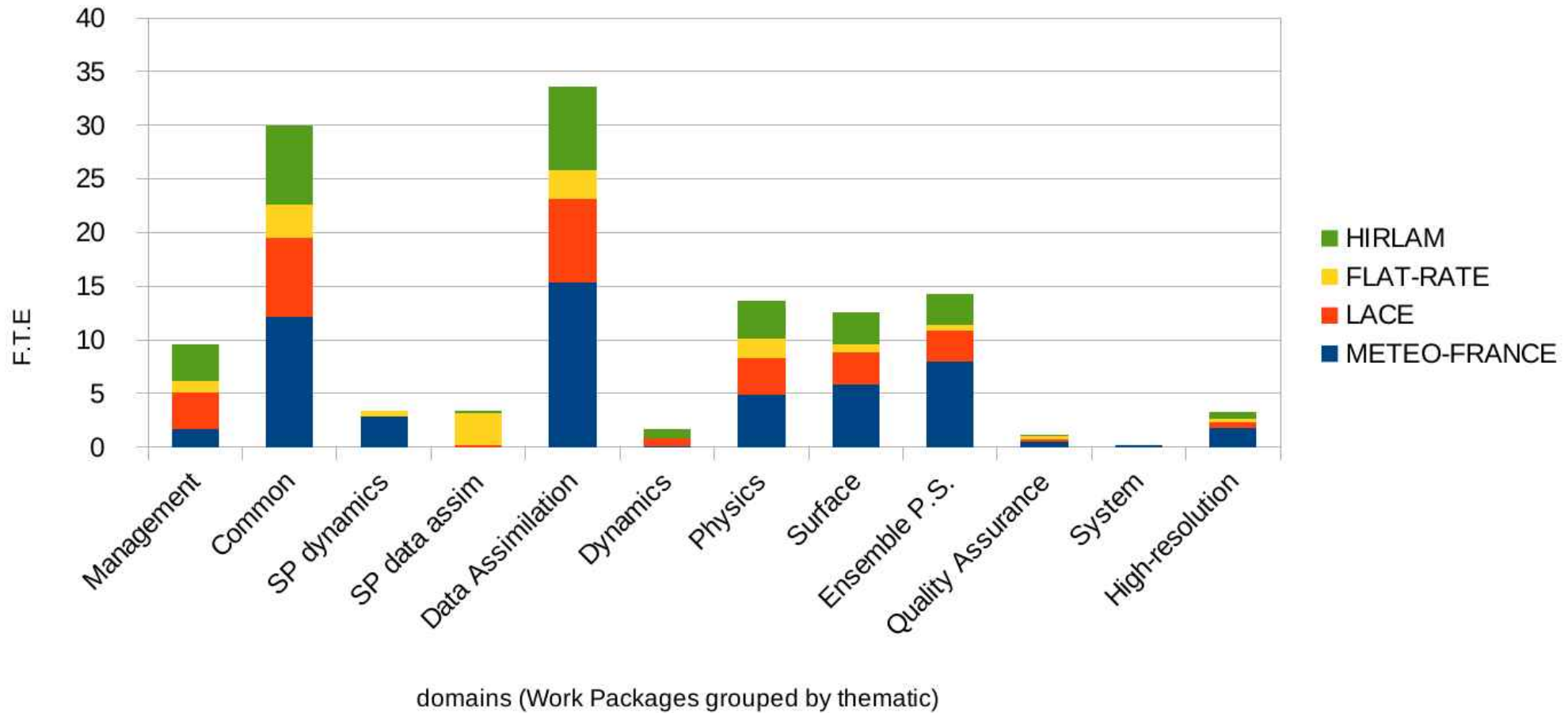


Prospective R&D activities :

Atmospheric data assimilation, Dynamics, Atmospheric physics parametrizations, Surface analysis and modelling, Probabilistic forecasting, Quality assessment and monitoring, Technical code and system development, Towards high-resolution modelling

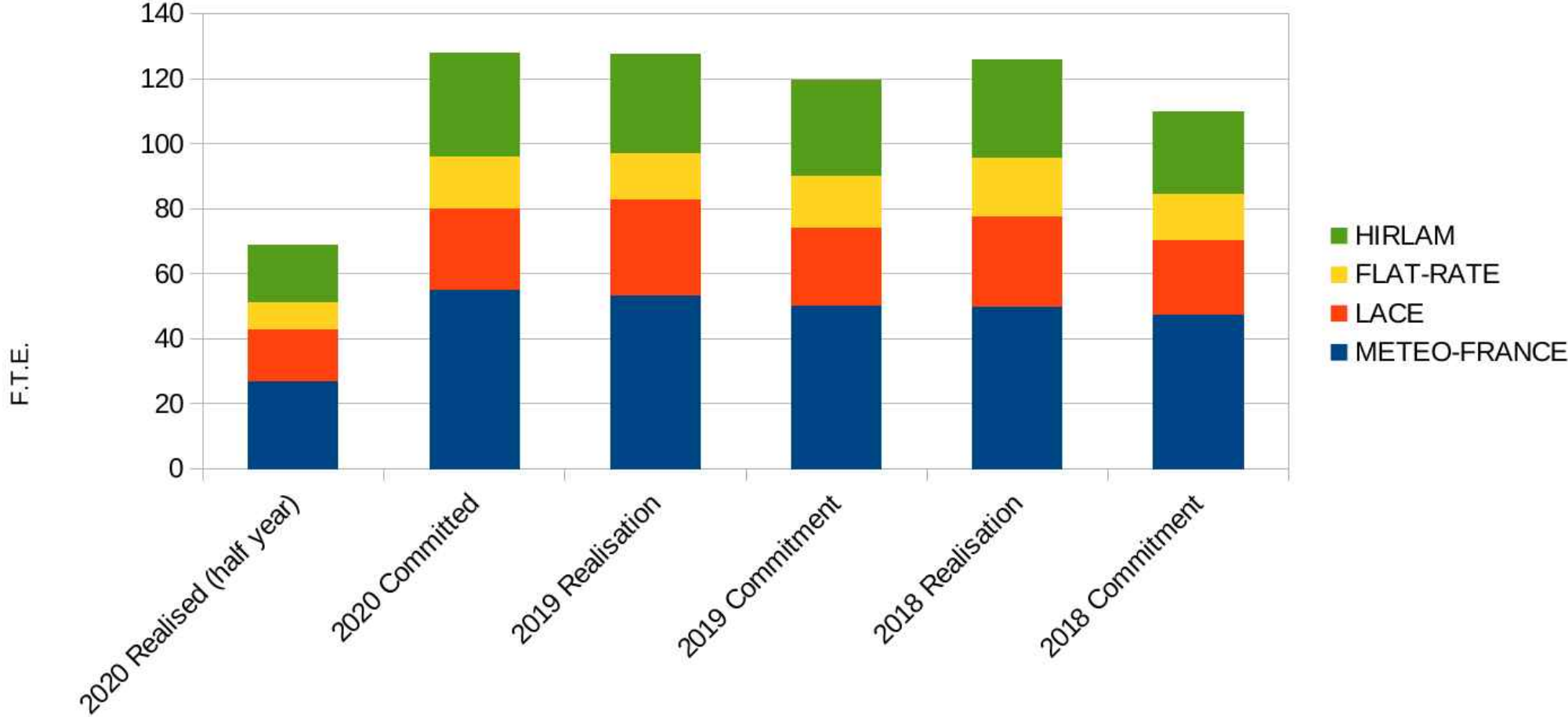
# Manpower reported in 2020 in each domain

breakdown by groupings



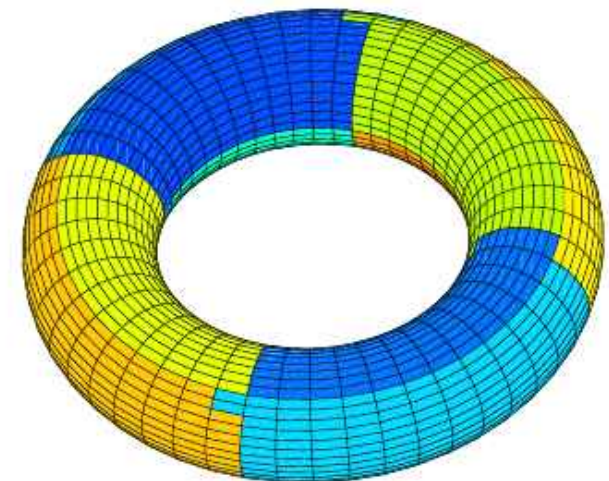
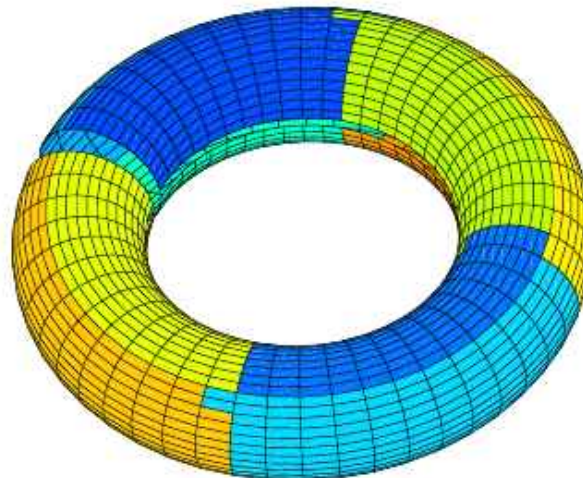
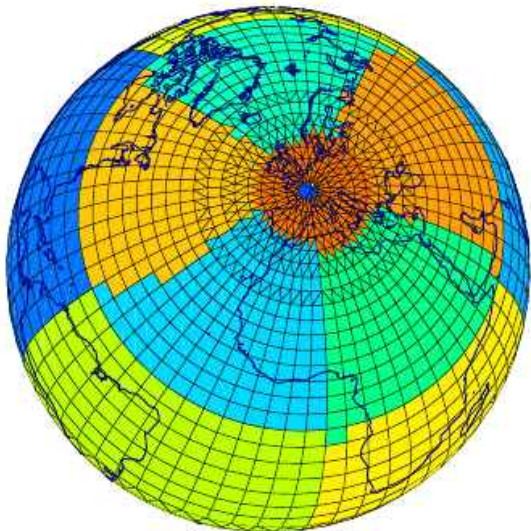
# F.T.E. in the Rolling Work Plans since 2018

Committed and reported figures, by groupings



# Transversal area: future evolution of software infrastructures

- Adopt the notion of “*separation of concerns*”: low level code to the local computing platform are not visible to the high-level scientific developer, thus separating the scientific concerns from the computing ones.
- Strengthen the collaboration with ECMWF (shared code)
- Work already started on Atlas to include LAM geometry
- Need to increase knowledge/efforts on DSL and Claw



Dynamics in LACE (working with current NH spectral core)

Vertical discretization: Design of VFE for NH model

Horizontal diffusion – Tuning and redesign depending on the scale

Dynamic definition of the iterative time schemes

Terms redistribution through new VV variables

Experiments in very high resolution

Optimization of the model code – single precision

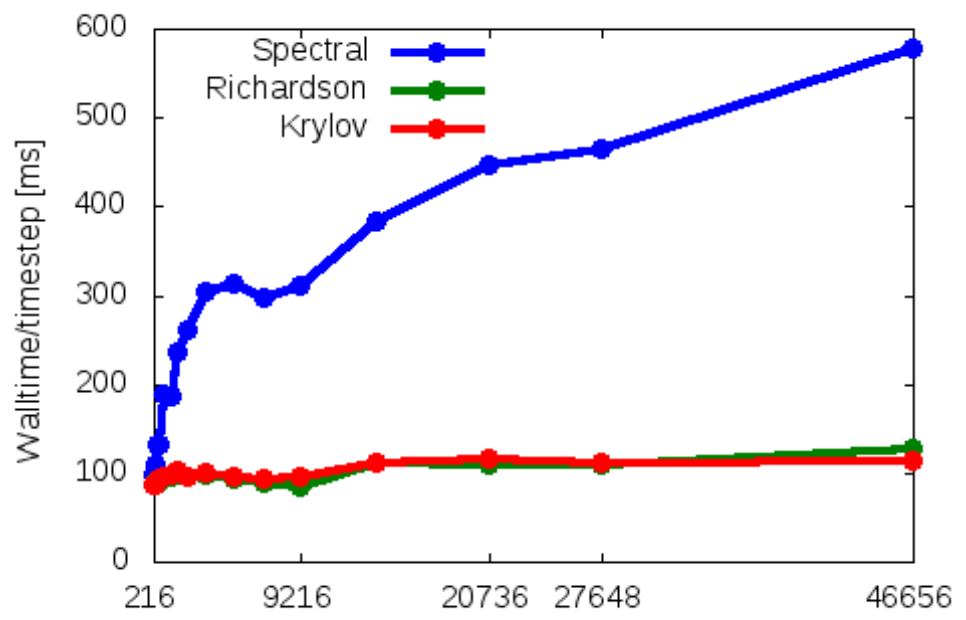
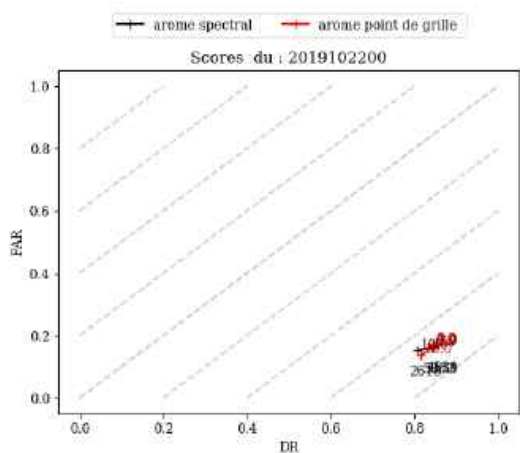
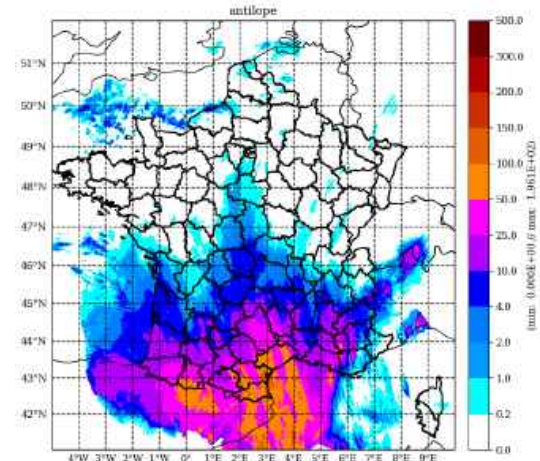
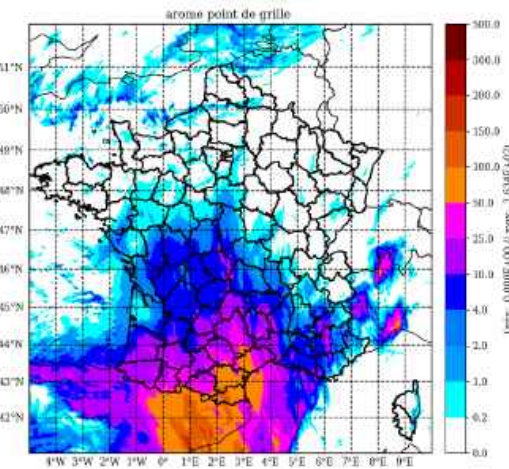
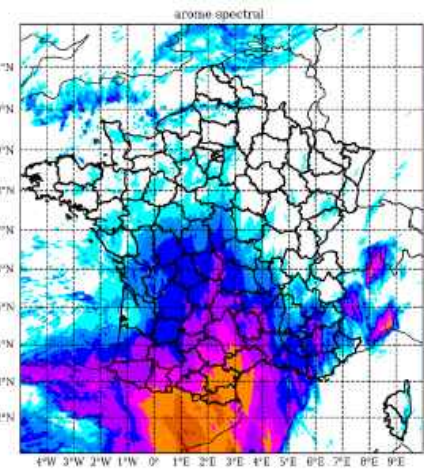
Coupling strategy, higher frequency

**Reformulation of the NH system as departure from HPE**

Nonhydrostatic dynamics was redesigned as pure increment to hydrostatic dynamics. Moreover, nonhydrostaticity may be introduced partially, depending on given parameters. Then an equilibrium between accuracy and stability may be found, where the results are very similar to full nonhydrostatic version and the stability is enhanced. For example, the corrector may be omitted and only one iteration time scheme may be used (SETTLS) in some cases where this was not possible with pure nonhydrostatic dynamics. (28th Aug to 23rd Oct 2020 Jozef Vivoda)

# Dynamics: a gridpoint solution

Step	Options (LAM vs. global)
1. Horizontal derivatives (vorticity, divergence and pressure-temperature gradients)	<ul style="list-style-type: none"> <li>bi-FFT<sup>-1</sup></li> <li>Legendre, FFT</li> </ul>
2. Inverse spectral transform: spectral to grid point	
3. Computation of the physics contributions	<ul style="list-style-type: none"> <li>AROME physics</li> <li>ALADIN/ALARO physics</li> <li>INTFLEX</li> <li>IFS-ARPEGE-ALADIN hydrostatic</li> <li>ALADIN-NH</li> <li>SLHD</li> </ul>
4. Calculation of the tendencies of the prognostic variables of the model state	
5. Computation of the explicit grid-point dynamics and adding it to the total tendencies of the prognostic variables	
6. Computation of the semi-Lagrangian departure points and Interpolation of the tendencies to these points	
7. Addition of the interpolated tendencies to the model state	bi-periodic LBC conditions
8. Lateral boundary coupling	
9. direct spectral transforms	<ul style="list-style-type: none"> <li>bi-FFT</li> <li>Legendre, FFT</li> <li>IFS-ARPEGE-ALADIN hydrostatic</li> <li>ALADIN NH</li> </ul>
10. solving the semiimplicit Helmholtz equation	



D. Degrauwe, C. Clancy

T. Burgot, L. Auger

## Tackling our biggest model problem: fog through realistic CCN/aerosol

### **Several of Harmonie's most aggravating forecast problems are connected:**

- too quickly growing, persistent, cold fog over sea
- radiation (cloudy) bias
- precipitation behavior in coastal zones

Fog behaviour is very sensitive to CCN amount/evolution. The model assumes too much cloud water. This also affects radiation/coastal precip behavior.

### Fundamental solution:

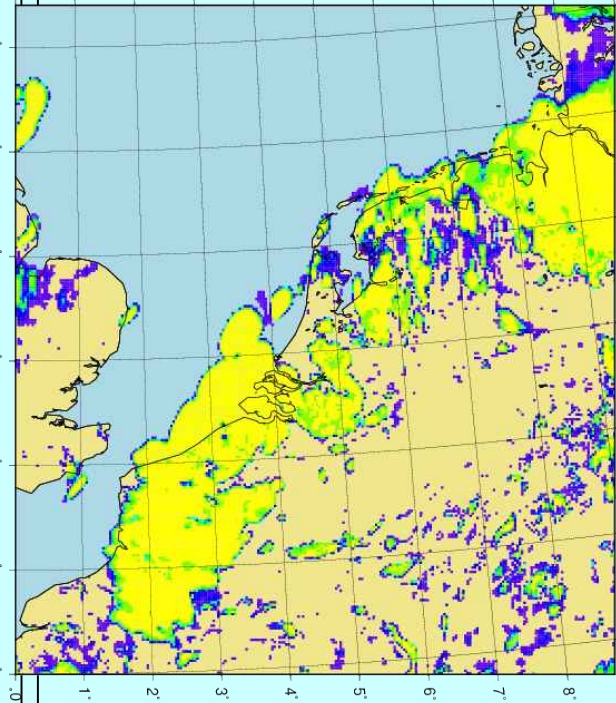
- Use 2d moment LIMA microphysics scheme to describe the evolution of CCN
- Initialize CCN and aerosols through CAMS
- Propagate the impact of CCN/aerosols to radiation/cloud schemes through aerosol parametrizations.

We have only just started to study LIMA. But we can already improve fog behavior a lot, using the present ICE3 microphysics and two small changes in the CCN concentration and LW radiation emissivity!

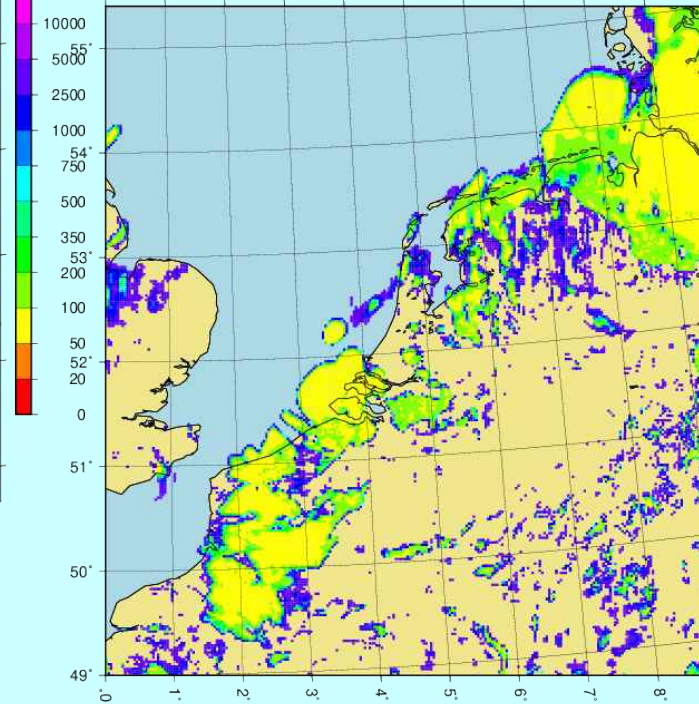


# Adjusting LW emissivity and CCN removes most spurious fog...

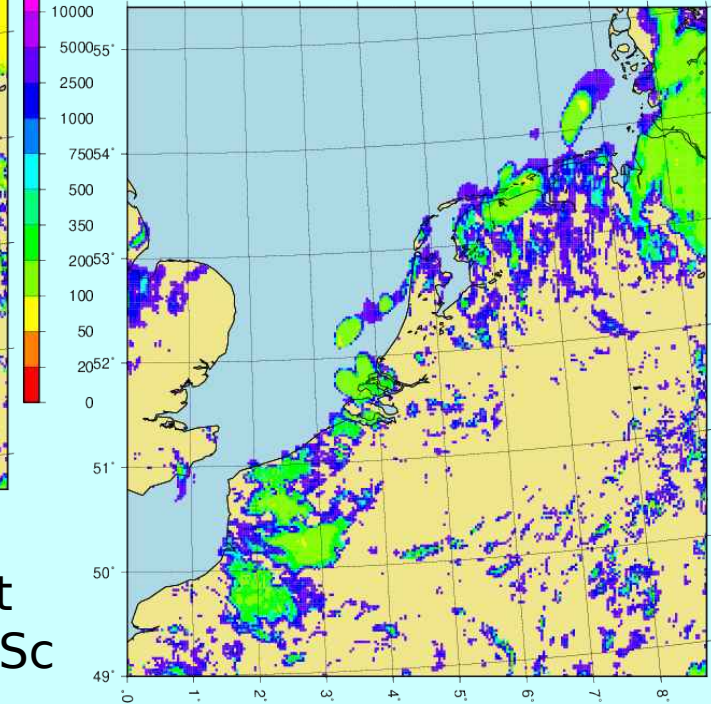
Vis 43\_tg1 2019032812+18



Vis 43\_tg1\_E 2019032812+18



Vis 43\_tg1\_E\_C 2019032812+18



... and gives more realistic cloud water path in most situations, but some degradation is seen in Cb and Sc  
... consider adaptation of supersaturation parametrization to better activate the CCN

## TOUCANS Third Order moments (TOMs) Unified Condensation Accounting and N-dependent Solver (for turbulence and diffusion)

The work on implementation of TKE-based mixing length in TOUCANS continued. In order to check the computation of BL89 integrals, the code was adapted to diagnose vertical parcel displacements ( $L_{up}$  and  $L_{down}$ ) from the ARPEGE subroutine *acb189.F90*. TOUCANS values were slightly smaller which is attributed to the impact of added shear term.

the meaning of  $L_{TKE}$  length scale (average of  $L_{up}$  and  $L_{down}$ )

the meaning of  $L$  and  $l_m$  length scales in TOUCANS is not as straightforward as it seemed

The main length scale  $L$ , which appears in TOUCANS equations, is equal to the Prandtl type mixing length in the free atmosphere, but in the surface layer it is increased by the factor  $\nu/C_K \approx 6$

$l_m$  and  $l_{gc}$  scales which also appear in TOUCANS equations have the meaning of the Prandtl type mixing length in the surface layer, while in the free atmosphere they correspond to the Prandtl type mixing length scaled by  $C_K/\nu \approx 1/6$

set  $L=L_{TKE}$  (or  $l_m=L_{TKE} \cdot C_K/\nu$ ). The smooth transition to  $L=\nu/C_K \cdot \kappa \cdot z$  in the surface layer is achieved by weighting

The scores for the winter inversion case were better than for the reference ( $l_{gc}$  mixing length) due to reduced mixing near the surface. However, during the convection there was not enough mixing above the surface layer and close to the top of the PBL.

Treatment of TTE (total turbulent energy) was improved to remove oscillations that occasionally appeared in the forecast, the computation is stabilized, leading to improved 2m temperature forecasts, the report is not available yet, but the researchers plan to publish the results in MWR.

# Physics developments in ALARO and AROME (including SURFEX)

The work on implementation of TKE-based mixing length in TOUCANS continued. the meaning of LTKE length scale (average of Lup and Ldown) the meaning of L and Im length scales in TOUCANS is not as straightforward as it seemed The scores for the winter inversion case were better than for the reference (lgc mixing length) due to reduced mixing near the surface.

Treatment of TTE (total turbulent energy) was improved to remove oscillations that occasionally appeared in the forecast, the computation is stabilized, leading to improved 2m temperature forecasts.

1) No melting case:

$$\alpha^{n+1} = \alpha^n - \text{TOLIN} \cdot \Delta t + \frac{F_{\text{snow}}}{\text{WNEW}} \cdot \Delta t, \quad (3.3)$$

where  $\text{TOLIN} = 0.008/86400 \text{ s}^{-1}$  is constant of aging of snow,  $F_{\text{snow}}$  is intensity of snowing and  $\text{WNEW} = 10 \text{ kg.m}^{-2}$ .

2) Melting case:

$$\alpha^{n+1} = \alpha^n - \text{TOEXP}(\alpha^n - \alpha_{\text{min}}) \cdot \Delta t + \frac{F_{\text{snow}}}{\text{WNEW}} \cdot \Delta t, \quad (3.4)$$

where  $\text{TOEXP} = 0.24/86400 \text{ s}^{-1}$  is constant of aging of snow in melting case and  $\alpha_{\text{min}} = 0.5$  is threshold for albedo of snow.

1) No melting case:

$$\alpha^{n+1} = \alpha^n - \text{XANS\_TODRY} \cdot \frac{\Delta t}{\text{XDAY}} + \frac{F_{\text{snow}}}{\text{XWCERN}} \cdot \Delta t \cdot (\alpha_{\text{max}} - \alpha_{\text{min}}),$$

where  $\text{XANS\_TODRY} = 0.008$  is aging of snow,  $\text{XDAY} = 86400$ ,  $F_{\text{snow}}$  is intensity of snowing,  $\text{XWCERN} = 10 \text{ kg.m}^{-2}$  and  $(\alpha_{\text{max}} - \alpha_{\text{min}}) = 0.35$ .

Replaced by

2) Melting case:

$$\alpha^{n+1} = \alpha_{\text{min}} + \exp\left[-\text{XANS\_T} \cdot \frac{\Delta t}{\text{XDAY}}\right] (\alpha^n - \alpha_{\text{min}}) + \frac{F_{\text{snow}}}{\text{XWCERN}} \cdot \Delta t \cdot (\alpha_{\text{max}} - \alpha_{\text{min}}),$$

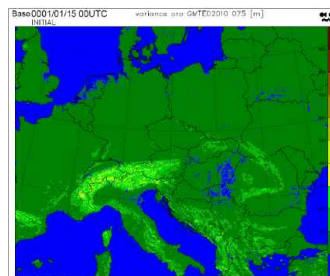
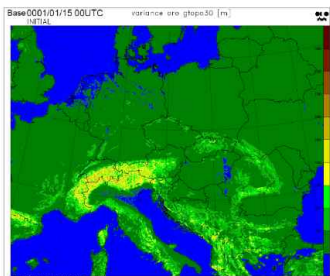
where  $\text{XANS\_TODRY} = 0.24$ .

For small  $\Delta t$ :

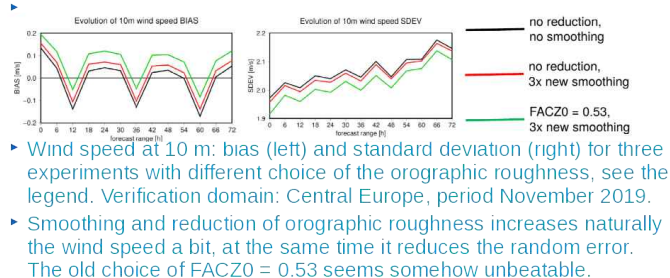
$$\alpha^{n+1} = \alpha^n - \text{XANS\_T} \cdot \frac{\Delta t}{\text{XDAY}} (\alpha^n - \alpha_{\text{min}}) + \frac{F_{\text{snow}}}{\text{XWCERN}} \cdot \Delta t \cdot (\alpha_{\text{max}} - \alpha_{\text{min}}),$$

Replaced by

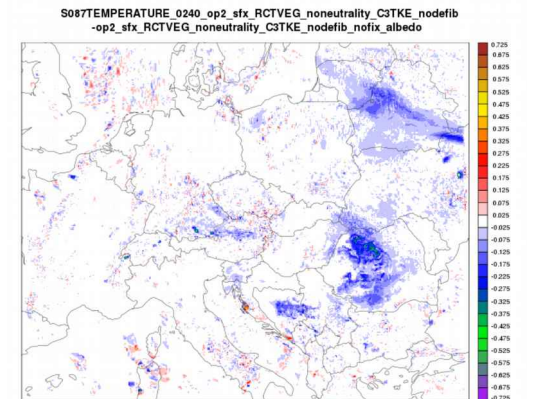
Replaced by



Left: orographic variance calculated from the old database GTOPO30. Right: orographic variance calculated from GMED2010 with 7.5" resolution. Model grid: 2 325 m.



- Wind speed at 10 m: bias (left) and standard deviation (right) for three experiments with different choice of the orographic roughness, see the legend. Verification domain: Central Europe, period November 2019.
- Smoothing and reduction of orographic roughness increases naturally the wind speed a bit, at the same time it reduces the random error. The old choice of FACZ0 = 0.53 seems somehow unbeatable.



# Physics

## Physically based stochastic perturbations and applied machine learning (AI)

Nonlin. Processes Geophys., 27, 187–207, 2020  
<https://doi.org/10.5194/npg-27-187-2020>  
 © Author(s) 2020. This work is distributed under the Creative Commons Attribution 4.0 License.



Nonlinear Processes  
 in Geophysics



### Simulating model uncertainty of subgrid-scale processes by sampling model errors at convective scales

Michiel Van Ginderachter<sup>1,2</sup>, Daan Degrauwe<sup>1,2</sup>, Stéphane Vannitsem<sup>1</sup>, and Piet Termonia<sup>1,2</sup>

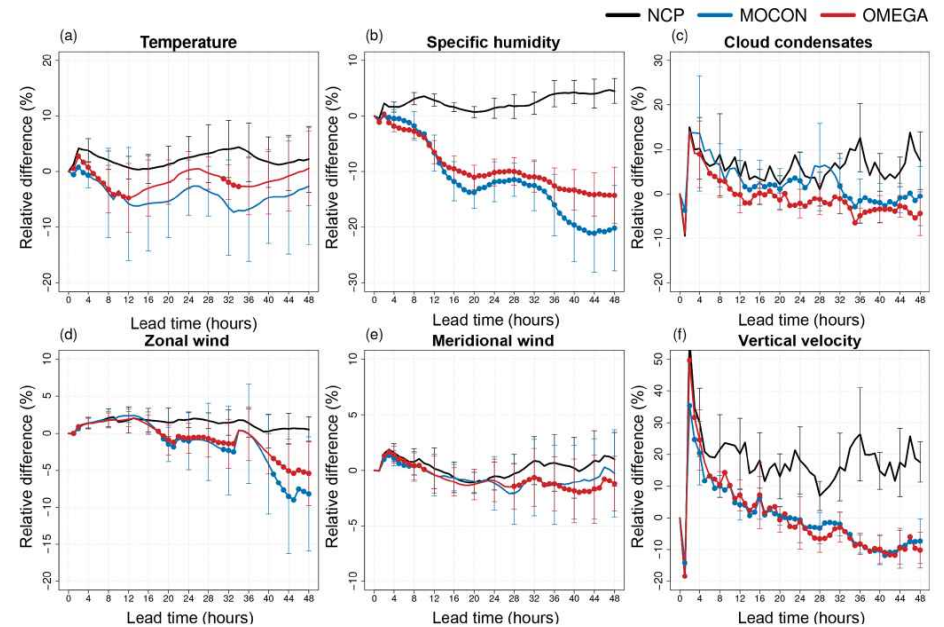
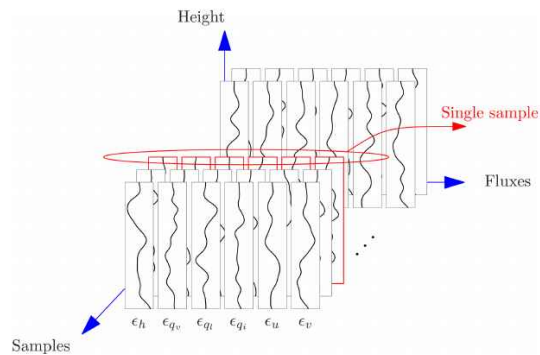
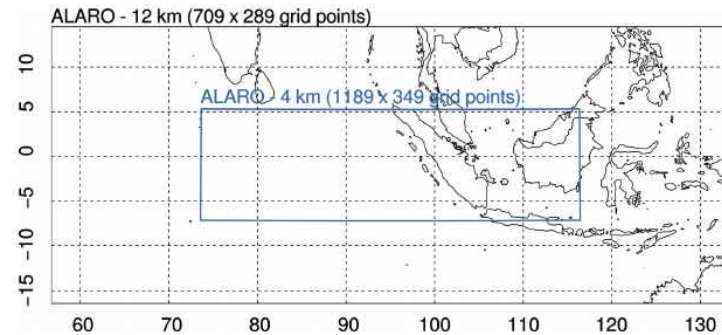
<sup>1</sup>Department of Meteorological Research and Development, Royal Meteorological Institute, Brussels, Belgium

<sup>2</sup>Department of Physics and Astronomy, Ghent university, Ghent, Belgium

Correspondence: Michiel Van Ginderachter (michiel.vanginderachter@meteo.be)

Received: 10 May 2019 – Discussion started: 24 May 2019

Revised: 24 January 2020 – Accepted: 24 February 2020 – Published: 16 April 2020

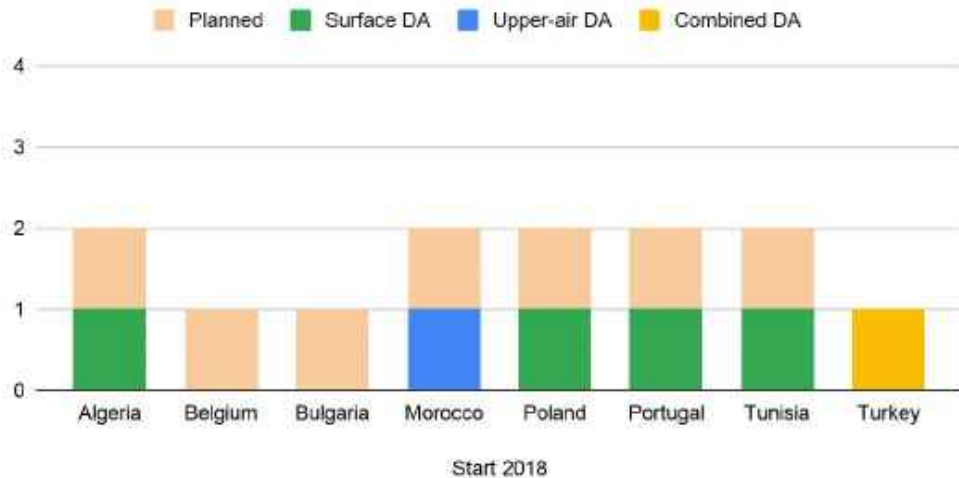


	No convection parameterization	With convection parameterization	Stochastic perturbation of model errors With random sampling			Machine learning
	NCP	Phys	PC5	PC10	PC20	GAN
RMSE	0.880	0.803	0.806	0.808	0.803	0.832
Bias	-0.308	-0.221	-0.225	-0.230	-0.222	-0.264
Spread	0.305	0.310	0.310	0.309	0.309	0.299
BS	0.272	0.233	0.234	0.236	0.233	0.247
BSS	-1.084	-1.006	-1.004	-1.009	-1.001	-0.994
RMSE	0.845	0.727	0.729	0.732	0.728	0.749
Bias	-0.303	-0.044	-0.048	-0.054	-0.044	-0.066
Spread	0.243	0.238	0.238	0.238	0.237	0.233
BS	0.322	0.215	0.217	0.219	0.216	0.234
BSS	-3.477	-1.313	-1.350	-1.395	-1.321	-1.711

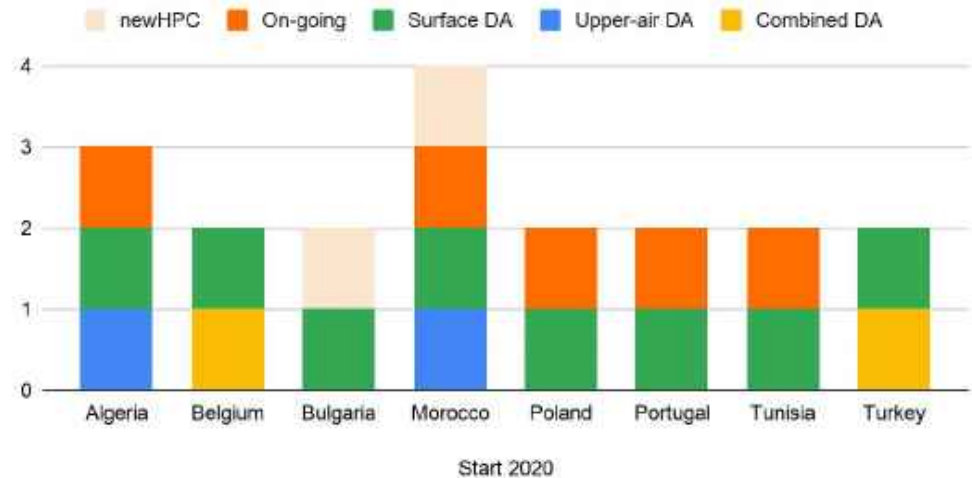
# Data assimilation: DAsKIT

Operational configurations		RUN OVER															
		Algeria	Belgium	Bulgaria	Morocco	Poland	Portugal	Tunisia	Turkey	Austria	Croatia	Czech Rep	Hungary	Romania	Slovakia	Slovenia	France
RUN BY	Algeria	ALADIN 12						ALADIN 12	ALADIN 12							ALADIN 12	
	Belgium		ALARO 4														
	Bulgaria			ALADIN 7													
	Morocco	ALADIN 18	ALADIN 18	ALADIN 18	AROME 2.5			ALADIN 10	ALADIN 18	ALADIN 18	ALADIN 18	ALADIN 18	ALADIN 18	ALADIN 18	ALADIN 18	ALADIN 18	ALADIN 18
	Poland		ALARO 4	ALARO 4		AROME 2.5					AROME 2.5	ALARO 4	AROME 2.5	AROME 2.5	ALARO 4	AROME 2.5	AROME 2.5
	Portugal								AROME 2.5								
	Tunisia															ALADIN 12	
	Turkey			AROME 2.5													AROME 2.5
	Austria										AROME 2.5	AROME 2.5	AROME 2.5	AROME 2.5		AROME 2.5	AROME 2.5
	Croatia										ALARO 8	ALARO 2	ALARO 8	ALARO 8		ALARO 8	ALARO 2
	Czech Rep			ALARO 4.7	ALARO 4.7		ALARO 4.7				ALARO 4.7	ALARO 4.7	ALARO 4.7	ALARO 4.7	ALARO 4.7	ALARO 4.7	ALARO 4.7
	Hungary			ALARO 8	ALARO 8		ALARO 8				ALARO 8	ALARO 8	ALARO 8	AROME 2.5	ALARO 8	AROME 2.5	AROME 2.5
	Romania				ALARO 6.5								ALARO 6.5	ALARO 6.5	ALARO 6.5		
	Slovakia			ALARO 9	ALARO 9		ALARO 9				ALARO 9	ALARO 9	ALARO 9	ALARO 9	ALARO 9	ALARO 9	ALARO 9
	Slovenia			ALARO 4.4							ALARO 4.4	ALARO 4.4	ALARO 4.4	ALARO 4.4		ALARO 4.4	ALARO 4.4
	France																

Combined DA, Upper-air DA, Surface DA and Planned - START 2018

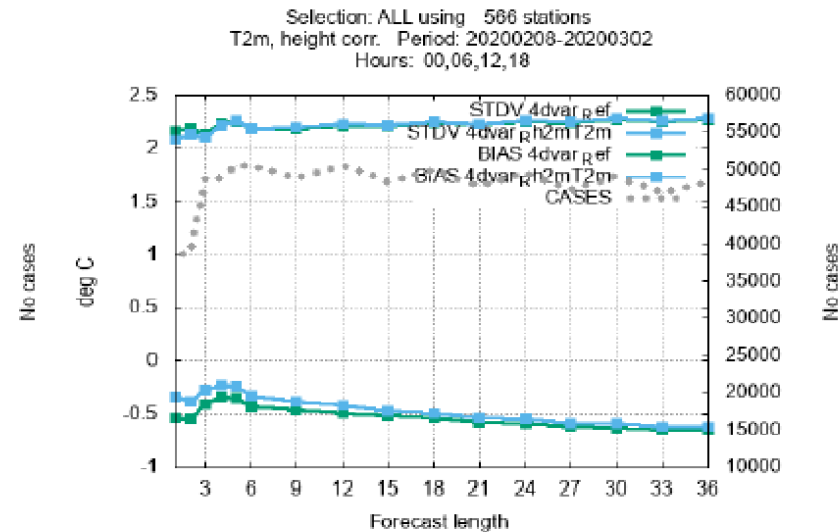
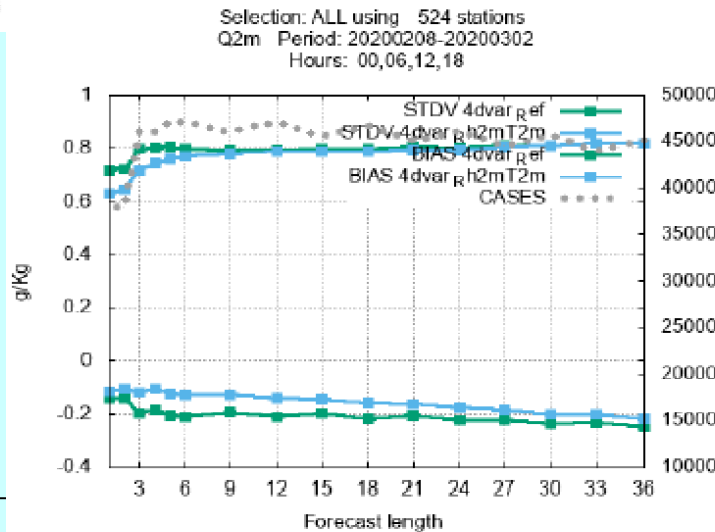
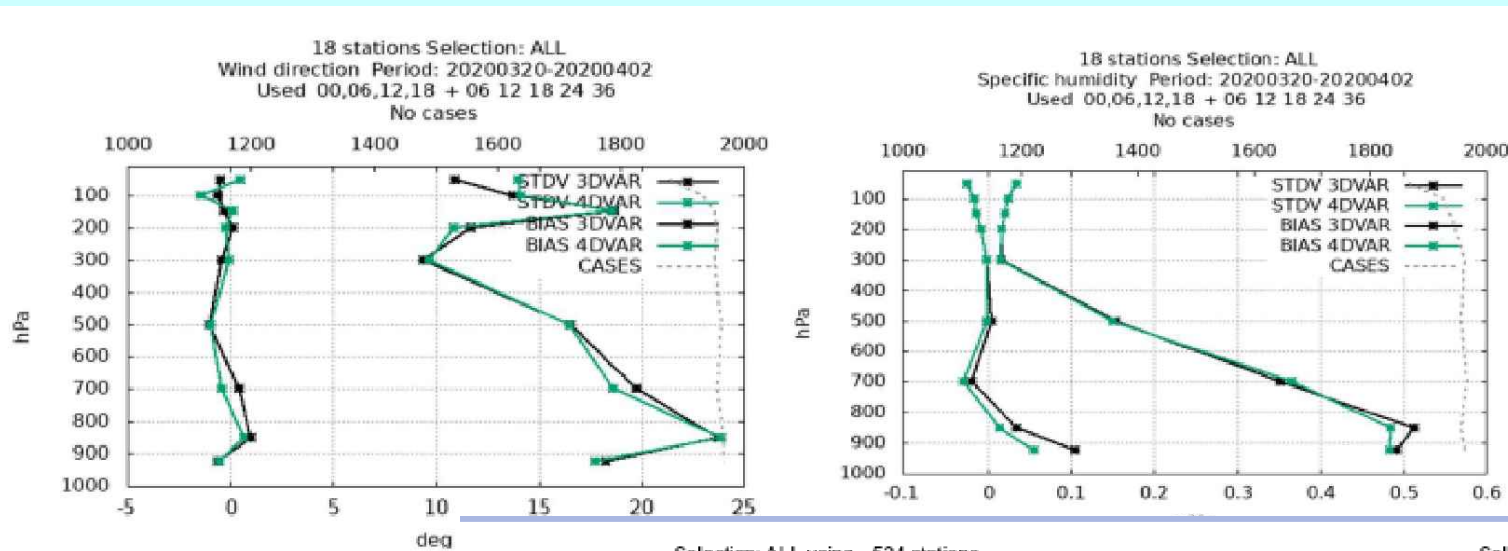


Combined DA, Upper-air DA, Surface DA, On-going and newHPC - START 2020



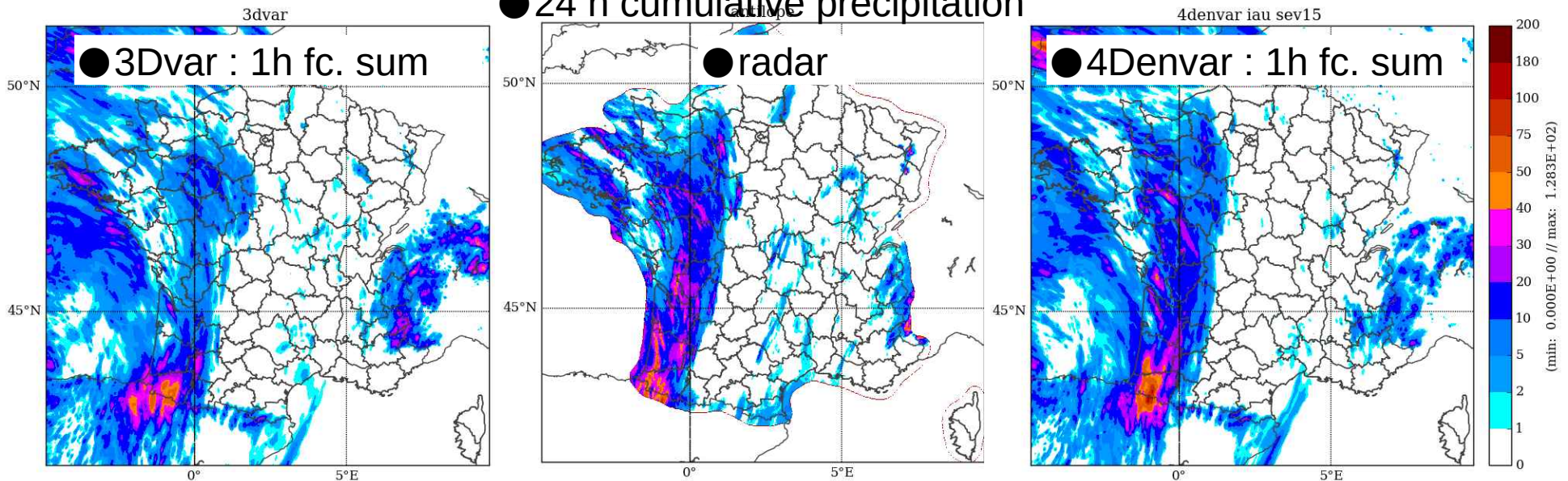
# Milestone: 4D-Var ready for operational use in Cy43h2.1.2

Extensive testing of 4D-Var on three domains, several combinations of observations and various 4D-Var settings, nearly concluded. Overall: 4D-Var as good as or slightly better than 3D-Var. Comp. cost ~ 12h forecast



# Tests with 4DenvVAR

● 24 h cumulative precipitation



$$J(\delta \mathbf{x}) = \frac{1}{2}(\delta \mathbf{x})^T \underline{\mathbf{B}}^{-1}(\delta \mathbf{x}) + \frac{1}{2}(\mathbf{d} - \underline{\mathbf{H}}\delta \mathbf{x})^T \underline{\mathbf{R}}^{-1}(\mathbf{d} - \underline{\mathbf{H}}\delta \mathbf{x})$$

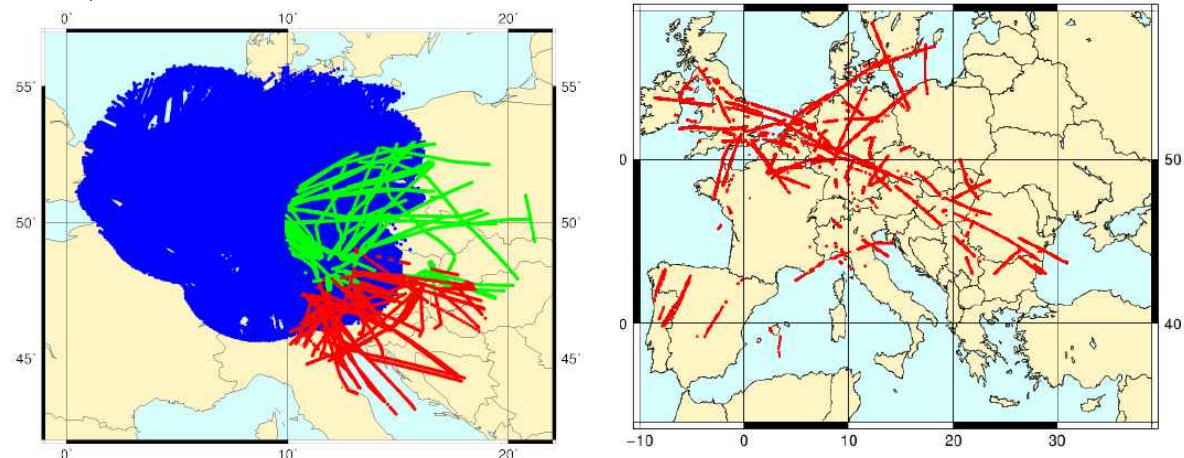
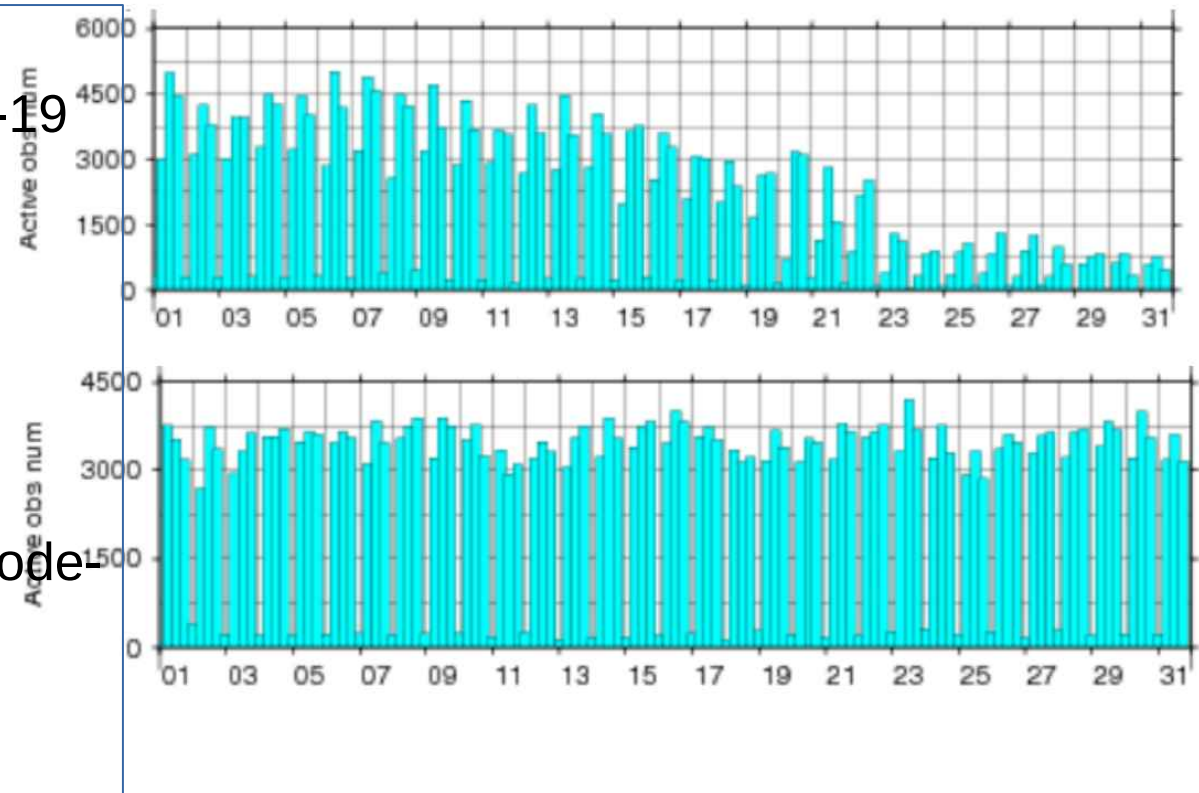
$$\underline{\delta \mathbf{x}} = \begin{pmatrix} \delta \mathbf{x}_0 \\ \delta \mathbf{x}_1 \\ \vdots \\ \delta \mathbf{x}_K \end{pmatrix}$$

$$\underline{\mathbf{B}} = \underline{\tilde{\mathbf{B}}^e} = \begin{pmatrix} \tilde{\mathbf{B}}_{0,0}^e & \tilde{\mathbf{B}}_{0,1}^e & \cdots & \tilde{\mathbf{B}}_{0,K}^e \\ \tilde{\mathbf{B}}_{1,0}^e & \tilde{\mathbf{B}}_{1,1}^e & & \tilde{\mathbf{B}}_{1,K}^e \\ \vdots & & \ddots & \\ \tilde{\mathbf{B}}_{K,0}^e & \cdots & & \tilde{\mathbf{B}}_{K,K}^e \end{pmatrix}$$

Desroziers et al. 2014

## Mitigation of reduced aircraft data for data assimilation

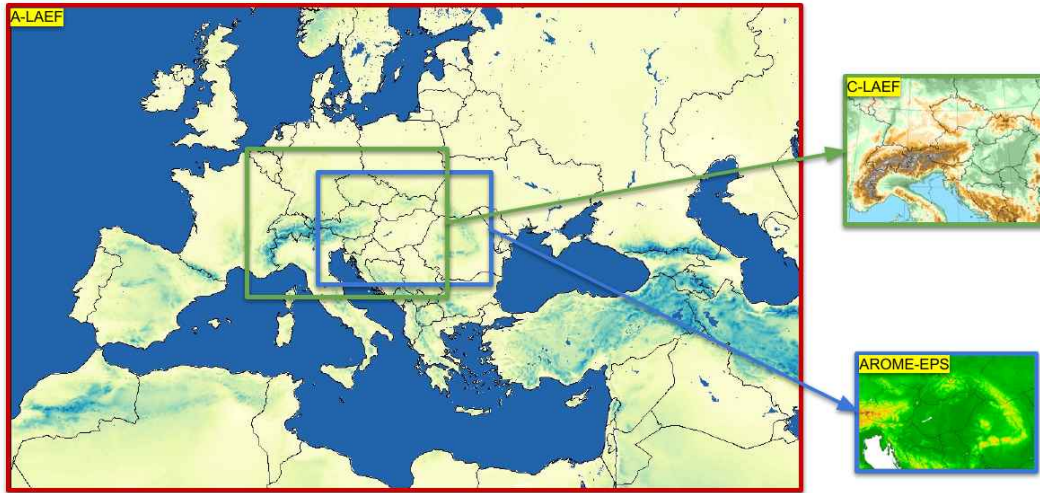
- decrease of aircraft observations due to COVID-19 in March 2020
- EUMETNET Observation Programme coordinated mitigating actions:
  - to increase radiosonde launch schedule
  - to enhance access to Mode-S data
- OPLACE processing of radiosonde data adjusted
- in August 2020 OPLACE contains around 80% of aircraft data from early March
- Additional ModeS data





# Operational ensembles of RC LACE

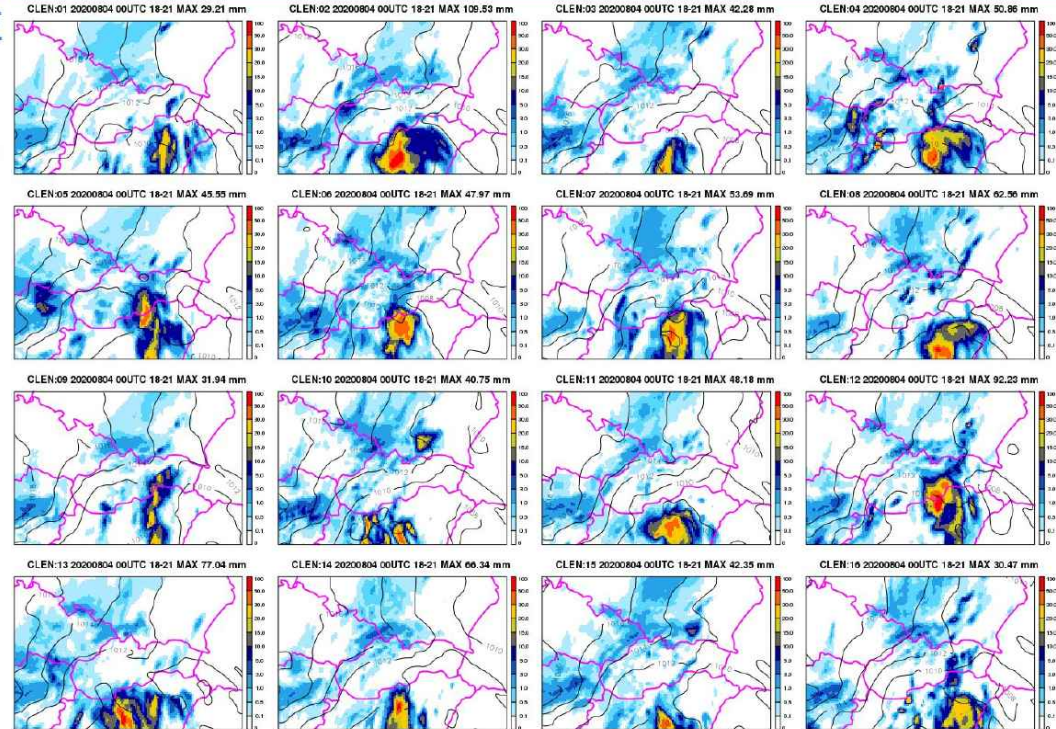
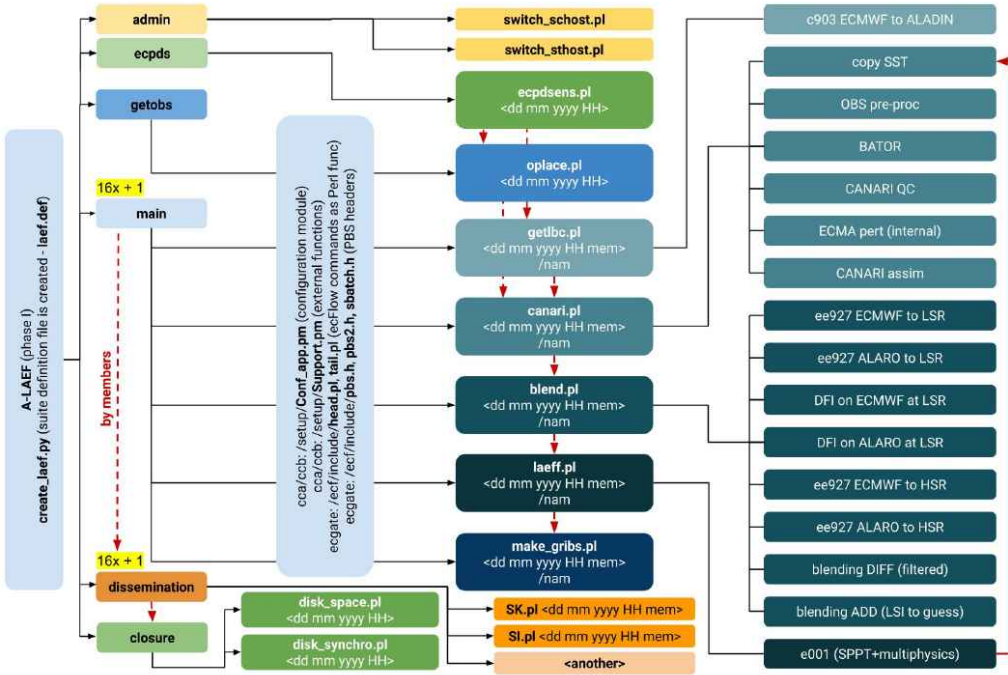
## Operational domains (in proper scale):



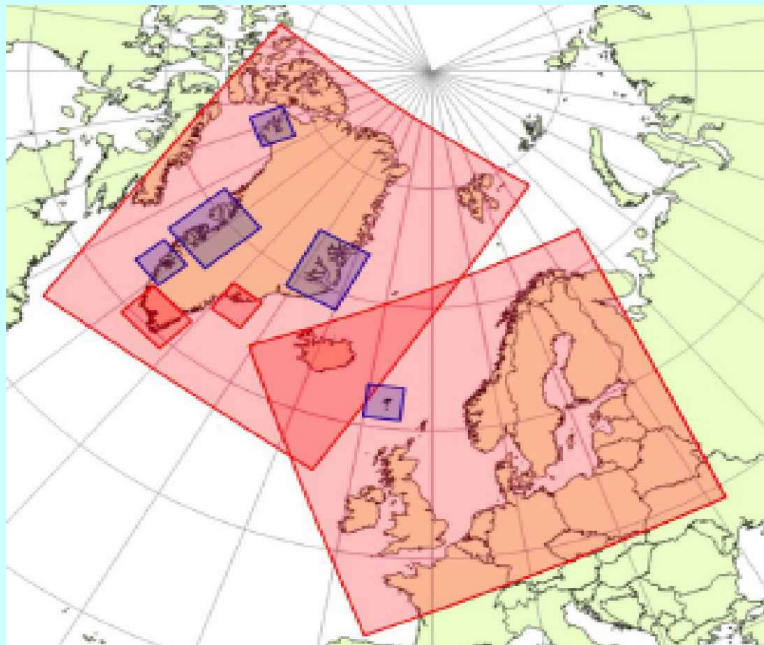
	A-LAEF	C-LAEF	AROME-EPS
CMC	ALARO	AROME	AROME
Code version	cy40	cy40	cy40
Horizontal resolution	4.8 km	2.5 km	2.5 km
Vertical levels	60	90	60
Runs per day	2	4	1
Forecast length	+72h (00/12 UTC)	+60h (00 UTC), +48h (12 UTC), +6h (06/18 UTC)	+48h (00 UTC)
Members	16+1	16+1	10+1
Assimilation cycle	yes (12h)	yes (6h)	-
IC perturbation	ESDA [surface], spectral blending by DFI [upper-air]	ESDA [surface], EDA, Ensemble-JK [upper-air]	downscaling (AROME-EDA is being tested)
Model perturbation	ALARO-1 multi-physics + surface stochastic physics (SPPT)	hybrid stochastic scheme with a combination of parameter and tendency perturbations	-
LBC perturbation	ECMWF ENS (c903@cy46)	ECMWF ENS (c901+e927)	ECMWF ENS (c903@cy47)

## A-LAEF (RC LACE)

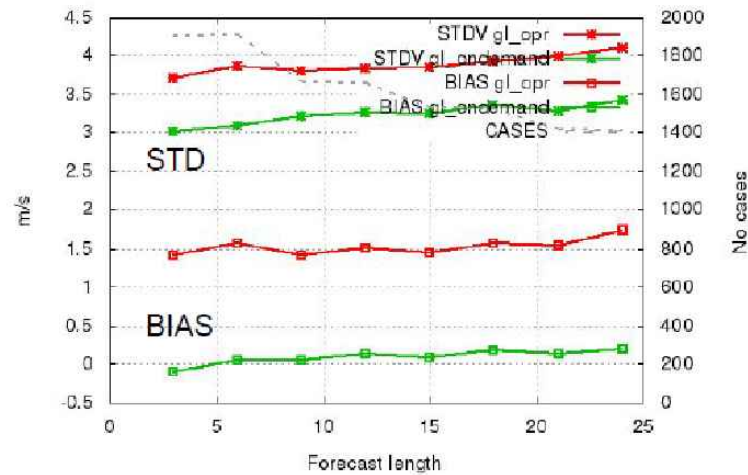
Regional Cooperation for Limited Area Modeling in Central Europe



# High-resolution models on-demand for warning purposes



Selection: ALL using 20 stations  
 U10m Period: 20200104-20200430  
 Hours: {00,03,...,21}

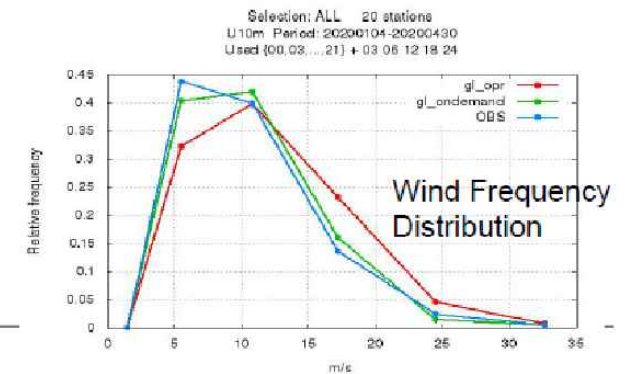
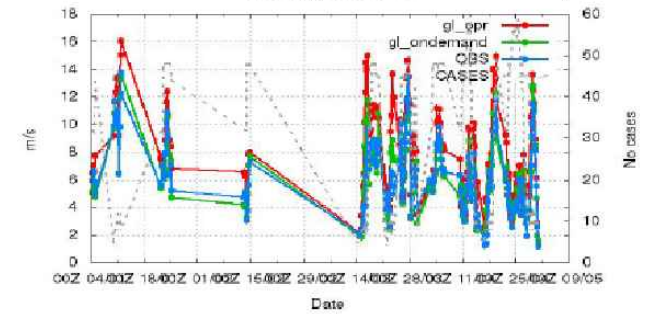


**Operational (IGB)**  
**HiRes On-demand**

Jan-April 2020

U10m  
 Selection: ALL 20 stations  
 Used {00,03,...,21} + 03 06 24  
 Averaging window: 6h

Daily averaged  
 Wind Speed



Wind Frequency  
 Distribution

Thank you for your attention!